Hybrid Method for Aerodynamic Shape Optimization in Automotive Industry

Frédérique MUYL[†], Laurent DUMAS[‡], Vincent HERBERT[† 1]

[†] *PSA Peugeot Citroën, Centre technique, 2 route de Gisy, 78943 Vélizy Villacoublay, France, Tel : (33)1 57 59 39 69 / 54 21, Fax : (33)1 57 59 21 77.*
[‡] *Laboratoire Jacques-Louis Lions, Université Pierre et Marie Curie, 175 rue de Chevaleret, 75013 Paris, France, Tel : (33)1 44 27 37 72, Fax : (33)1 44 27 72 00.*

Abstract

An aerodynamic shape optimization tool for complex industrial flows is developed, based on an hybrid process. The optimization method couples a stochastic genetic algorithm and a deterministic BFGS hill-climbing method. For each evaluation required by the optimizer, the Navier-Stokes equations with the $k-\epsilon$ turbulence model are solved with a commercial CFD code on an unstructured mesh surrounding the shape to optimize. After various validation test cases, the method is successfully applied to optimize the rear of a simplified car shape in order to bring acceleration in the computational time of the minimization of the drag coefficient.

Keywords : genetic algorithms, hybrid method, CFD, shape optimization.

Introduction

Decreasing the fuel consumption of road vehicles, due to environmental and selling arguments reasons, concerns car manufacturers. Consequently, the improvement of the aerodynamics of car shapes, more precisely the reduction of their drag coefficient, becomes one of the main topics of the automotive research centers. As it has been shown that forty per cent of the drag coefficient depends on the external shape ([1]) and most of it on the rear of the geometry, a numerical optimization process is proposed here in order to seek innovative low-drag car shapes. The main objective of this study is to set up an optimization strategy for mono-disciplinary design problem using fluid mechanics analysis. The automatic method of optimization developed in this paper is based on the coupling of two types of algorithms, a stochastic and a deterministic one.

The stochastic algorithm chosen is a Genetic Algorithm (GA). In order to reduce its prohibitive simulation time while keeping its advantages, it has been coupled with a deterministic gradient-based method which has the advantage to converge rapidly to a local solution, in the following way: first, a random population of solutions is improved by means of a GA. Then, few steps of a gradient-based method are applied to the best individual obtained by the GA. This new individual is re-injected into the population and the GA restarts until its next *plateau*. The hybrid algorithm is stopped after stabilization of the solution. The genetic process is just slightly perturbed but in the same time, the gradient method allows a quicker descent to the optimal solution.

In industrial applications, one of the difficulties of gradient-based methods is the computation

[1] *E-mail :* frederique.muyl@mpsa.com, dumas@ann.jussieu.fr, vincent.herbert@mpsa.com

of the sensitivity of the cost function with respect to its parameters. As a commercial CFD code has been used to solve the incompressible Navier Stokes and $k-\epsilon$ equations, a finite differences approximation of the gradient has been experimented here.

The paper is divided into three parts. First, some particularities of the optimization methods are introduced. Then, the new hybrid method is validated through analytic optimization. Finally, some results are presented for a first 3D shape optimization.

1 Optimization methods

1.1 Genetic Algorithms

The Genetic Algorithms are optimization methods inspired from the Darwinian theory of species improvement ([2], [3]). A population of potential solutions of the optimization problem is generated and evolves through the three natural principles which are selection, crossover and mutation. As this method does not require any particular regularity of the cost function, it can be applied to any optimization problem. Moreover as the GA's are global methods of optimization, they seek a global optimum; they are also able to solve multi-objective problems and are easily parallelizable.

To understand more precisely the mechanism of GA's, we consider the problem of minimizing a cost function J, depending on the parameter x lying in a convex search space called E, for instance an hypercube of $\Re^p$. We define a positive fitness function $x \mapsto f(x)$ inversely proportional to J to traduce how good the potential solution x is. The initial population consists in a collection of n potential solutions of the problem randomly chosen in E. We apply to this population a set of genetic operators that create a renewed population after each generation of the process : the individuals could either survive, reproduce or die according to their fitness value. The genetic operators that keep our interest in such technique are selection, crossover and mutation. As many types of each operator exist, we only present below those we used in our algorithm.

The selection consists here in a roulette-wheel slot where each potential solution is represented proportionally to its fitness rank in the population. A new population is created by spinning the wheel n times, where n is the population size.

The crossover is used to create new individuals from a pair of individuals, x and x', in order to increase diversity among the population. In our case, it is applied with a probability $p_c = 0.9$ and consists in an independent barycentric mixing of each real coordinate of x and x'.
The mutation operator is needed for a local exploration of the search space. Here, the mutation acts with a probability $p_m = 0.3$ and is called non uniform, because the more the GA is running, the weaker its average exploration range becomes.

To end an iteration of the GA, the new individuals thus obtained (called offsprings) are evaluated and replace the old ones (called parents) with the only exception of the previous best individual that is always kept in the new population (1-elitism).

Because of their simplicity and robustness, the GA's are more and more used in engineering applications ([3]). However, their weakness stays in their great requirement of cost function evaluations that can be very time consuming, as happens for aerodynamic optimization application where the solution of a complex partial differential equations system is necessary. Moreover, they don't permit a fine convergence to the solution. Thus, coupling a GA with a faster local optimization technique appears to be an effective way to overcome this lack of efficiency while keeping the advantages of this method.

1.2 A new hybrid method

The introduction of hybrid methods comes from the need to tackle more and more complex industrial applications whose resolution becomes unpractical with GA optimization technique. There exists different strategies to improve the efficiency of stochastic optimization methods. For instance, Vicini ([4]) and Poloni ([5]) propose a hybridization of the genetic operators by allowing a hill-climbing process (respectively, a conjugated gradient and a Powell method) between selection and crossover.

In this study, the hybrid method doesn't disturb as much the stochastic process. The hill-climbing method is just introduced every time after a stagnation in the GA has been observed during two consecutive generations. It consists in applying few steps of a quasi-Newton method using the BFGS (Broyden-Fletcher-Goldfarb-Shanno) approximation of the hessian matrix. Only the best individual of the current generation is improved in order not to disturb too much the stochastic algorithm. This acceleration process is repeated until a stabilization of the best solution is reached.

Before showing the results obtained for aerodynamic 3D shape optimization, the method has been validated with two analytic optimization test cases presented below.

2 Validation of the new hybrid method

In order to determine the efficiency of the previous new hybrid technique, we perform the minimization of two analytic functions : the Rastrigin function which exhibits many local minima but only one global minimum, and the Griewank function defined respectively as :

$$J_R(x_1, \cdots, x_p) = \sum_{i=1}^{p} \Big(x_i^2 - \cos(18 x_i) \Big) + p$$

and

$$J_G(x_1, \cdots, x_p) = \sum_{i=1}^{p} \frac{x_i^2}{50} \quad - \quad \prod_{i=1}^{p} \cos\left(\frac{x_i}{\sqrt{i}} \right) + 1$$

which both admit a global minimum for $(x_1, \cdots, x_p) = (0, \cdots, 0)$.

We consider the optimization of the Rastrigin function with 20 parameters and the optimization of the Griewank function with 50 parameters. The search spaces are respectively defined by $[-5, 5]^{20}$ and $[-20, 20]^{50}$. For each problem, we compare the results obtained by a deterministic, a genetic and a hybrid process.

Figures 1 and 2 show the convergence history with respect to the number of cost function evaluations. During the deterministic phases, the evaluation of a gradient counts for p evaluations, where p is the number of optimization parameters.

For the Rastrigin function, the global minimum is approached with the same level of accuracy after 1700 evaluations with the hybrid method compared to 400000 evaluations for the GA. On the other hand, the BFGS method alone doesn't permit to find the global optimum of the problem even with many different initial points (it is generally trapped in a local minimum).

For the Griewank function, to attain the same level of accuracy, the hybrid method uses 400 evaluations against 200000 for the stochastic method.

According to the previous encouraging results of the hybrid method on analytic cases, it has then been applied on an aerodynamic 3D shape optimization.

3 Aerodynamic shape optimization

3.1 Description of the optimization problem

We consider a vehicle-like body in ground proximity (see figure 3). The simplified car shape can be decomposed in a forebody, a midsection and an afterbody shape. The afterbody shape is defined by the three independent angles (the back-light angle α, the boat-tail angle β and the ramp angle γ). The afterbody length is equal to 15% of the total body length and the height of the body is equal to 40% of the body length. The problem is to minimize, by varying the three afterbody angles, the drag coefficient of the body called C_x and defined by :

$$C_x = \frac{2F_x}{\rho V_\infty^2 S}$$

where ρ is the mass density, S the front surface, V_∞ the freestream velocity and F_x the longitudinal component of the aerodynamic force defined by :

$$\vec{F} = \iiint_{Shape} P_{rel}\vec{n}dS + 2\mu \iiint_{Shape} D\vec{\nu}dS$$

where P_{rel} is the pressure around the shape relatively to the atmospheric pressure, $\vec{n}$, the normal vector, $\vec{\nu}$ the unit projection of the velocity vector to the surface, μ the dynamic viscosity and D the wall shear stress tensor.

In fact, most of the drag on a vehicule-like body comes from the pressure term and is directly due to flow separation from the body surface. While it is often observed that the drag coefficient is not sensitive to the forebody shape (with separation-free forebodies), flow separation, i.e. vortex shedding of longitudinal edges on the afterbody, is the major source of aerodynamic drag for vehicle-like body (see figure 5). Thus, the variation of the back-light angle, will modify the complex and higly nonlinear aerodynamic interaction among the upper, side and lower surfaces, leading different afterbody vortex structures creation impacting directly on the drag coefficient value.

The drag coefficient of the vehicle-like body is evaluated by numerical computations performed with a commercial 3D finite volume based solver, using the Navier-Stokes equations with $k-\epsilon$ turbulence model. The jamming surface is approximately equal to 1%. The numerical wind tunnel length is equal to nine vehicle lengths, two lengths upstream and six downstream. Symmetric boundary conditions are enforced at the symmetry plane. The mesh around the shape is unstructured and tetrahedral with about 350000 cells. A log-law boundary condition is employed on the car shape and on the wind tunnel ground.

For all the computations, the freestream velocity is equal to $40m/s$, which corresponds to a Reynolds number based on the body length of 3.5 10^6.

The convergence is assumed after stabilization of the drag and lift aerodynamic coefficients. Concerning the sensitivity evaluations, a specific study of the numerical stability and accuracy permits to determine the discretization step for the finite differences computations.

3.2 Results

Before showing the results, the optimization based on the hybrid method is described. The GA is running during five generations but it evolves only at the third one. Then the deterministic method is applied to the current best individual. The GA restarts just for three generations and the deterministic process is used again. Figure 4 presents the results obtained with the GA and the hybrid method. The drag coefficient values are plotted with respect to the computational

time for one CPU. Thus, the hybrid method permits to minimize the drag coefficient more efficiently than the GA in less than 70% of its computational time.

To interpret the mechanisms modifying the drag coefficient, two different view points, either aerodynamic or "geometric", can be taken ([6]) : on an aerodynamic view point, it has been observed by Morelli ([7]) and Hucho ([1]) that minimizing the trailing vortices in the wake will reduce drag. On a geometric view point, it seems to be interesting to minimize the rear base to reduce the drag. Indeed, it is worth noticing that the main changes on the drag when changing the shape deal with the pressure force. Moreover, as only 30% of the drag coefficient depends on the front of the shape, the slanted surfaces and vertical base surface of the rear end will contribute strongly to the pressure drag.

Unfortunately, both theories can't be considered separately. Indeed, a little rear base exists when the three rear angles have a high value but the latter induce important recirculation on the back-light, boat-tail, ramp faces which, as we have seen before, is a direct production of drag. Thus, a 3D Navier-Stokes analysis is applied in order to explain the flow associated to the optimized shape.

To illustrate the aerodynamic optimization, we present two computational results in the symmetry plane and in the middle transverse plane for two different shape configurations with an decreasing drag : (α, β, γ) equal to $(14.5, 7.6, 14.3)$ and (α, β, γ) equal to $(23.1, 13.6, 23.3)$. On figure 6, the wake behind the body is characterized by a large recirculation zone. At the symmetry plane two vortices are clearly visible. The separation bubble has a length slightly greater than a third of the vehicle length. The large flow separation on the rear base permits to predict a large contribution of this part to the pressure drag. The second shape depicted on figure 7 presents a 0.023 weaker drag. The rear base surface is indeed smaller than before and the effect of the back-light, ramp and boat-tail angles tends to minimize the length of the separation zone as well as the rear vortices intensity. The flow behind this shape is characterized by two well balanced upper and lower recirculation vortices in the separation bubble and the longitudinal vortices downstream are minimized. This flow is a typical low drag vehicle flow.

Conclusion

This study presents a new approach for global aerodynamic optimization problems. The Genetic Algorithms have been extensively used for that case but are very time consuming in a real industrial context. The coupling of a GA with a deterministic method has been introduced in this article in order to bring acceleration in the computational time and thus allow to handle complex 3D optimization problems.

The new hybrid method has been first validated on academic test cases. Then, an application in the automotive aerodynamic context has been investigated on which it has shown satisfactory results in terms of speed and efficiency compared to other existing methods. A 3D Navier-Stokes analysis shows that the flow around the vehicle-like shape optimized by the hybrid method is characteristic of a low drag vehicle flow.

The hybrid method can still be improved using partial automatic differentiation for the gradient evaluations rather than a finite differences approximation whose computational time depends on the number of optimization parameters, that could rapidly become an important drawback.

References

[1] HUCHO. *Aerodynamics of road vehicles.* Wolf-Heinrich HUCHO, 4th edition, 1997.

[2] D. E. GOLDBERG. *Algorithmes génétiques.* Addison-Wesley, 1991.

[3] B. STOUFFLET B. MANTEL E. LAPORTE J. PERIAUX, M. SEFRIOUI. *Robust Genetic Algorithms for optimization problems in aerodynamic design.* in Genetic Algorithms in engineering and computer science, John Wiley and Sons Ltd, 1995.

[4] A. VICINI and D. QUAGLIARELLA. *Airfoil and wing design through hybrid optimization strategies.* AIAA paper, 1998.

[5] C. POLONI. *Hybrid GA for multi objective aerodynamic shape optimization.* in Genetic algorithms in engineering and computer science, John Wiley and Sons Ltd, 1995.

[6] C.J. SAGI T. HAN, D.C. HAMMOND. *Optimization of bluff body for minimum drag in ground proximity.* AIAA paper, april 1992.

[7] A. MORELLI. *Aerodynamic basic bodies suitable for automobile applications.* Interscience Enterprise Ltd, 1983.

[8] M. YOSHIMOTO S. HARUNA T. NOUZAWA, K. HIASA. *Influence of the geometry of rear part on the aerodynamic drag and wake structure of a vehicle.* Mazda Motor Corp.

Figures

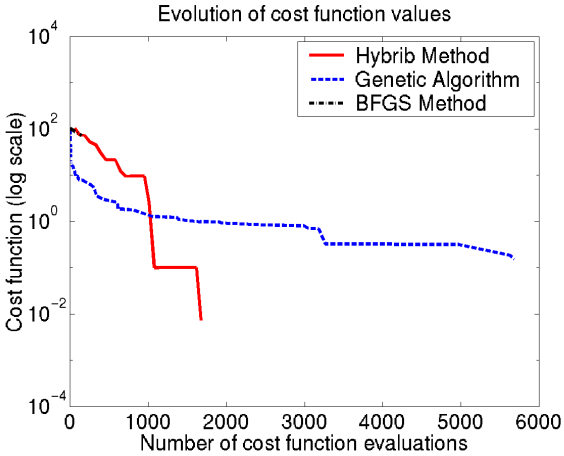

Figure 1: Convergence results for the optimization of the Rastrigin function with 20 parameters.

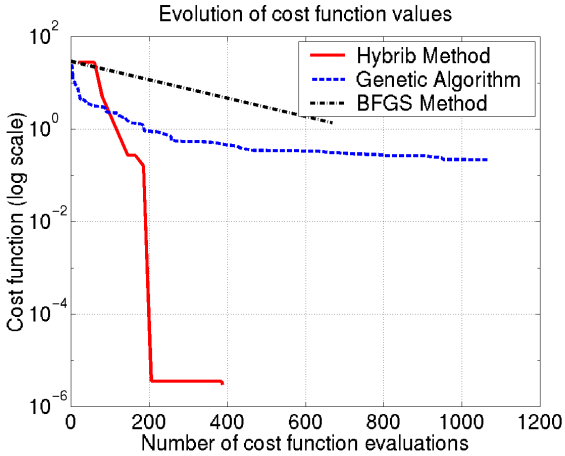

Figure 2: Convergence results for the optimization of the Griewank function with 50 parameters.

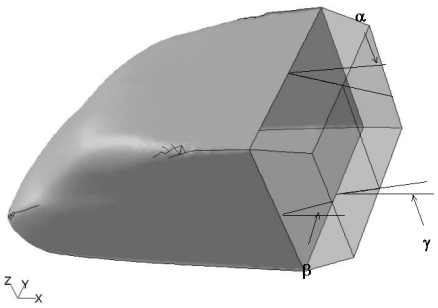

Figure 3: 3D car shape where the back-light angle called α, the boat-tail angle called β and the ramp angle called γ are adjustable.

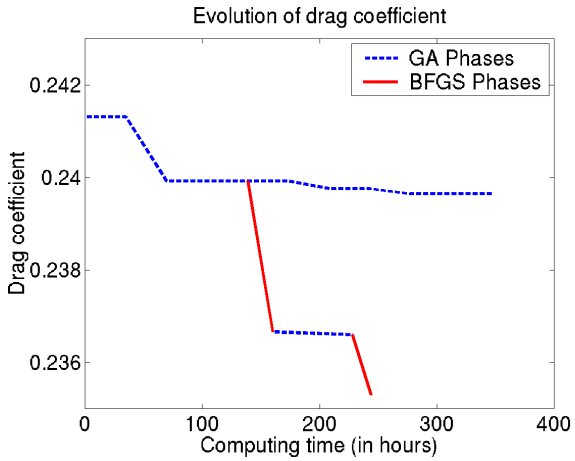

Figure 4: Convergence results for 3D shape optimization with 3 parameters.

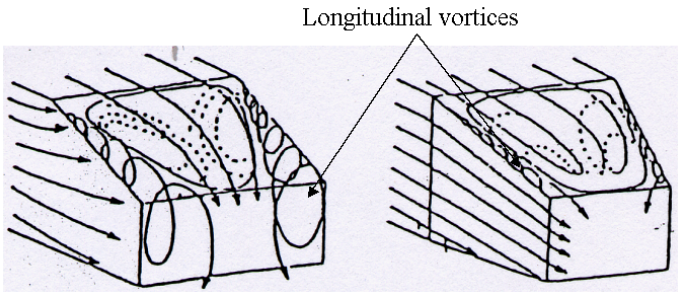

Figure 5: Schematic sketch of a vehicle-like body rear end flow (issued from [8]). *Left:* strong longitudinal vortices corresponding to a high drag. *Right:* weak longitudinal vortices corresponding to a low drag.

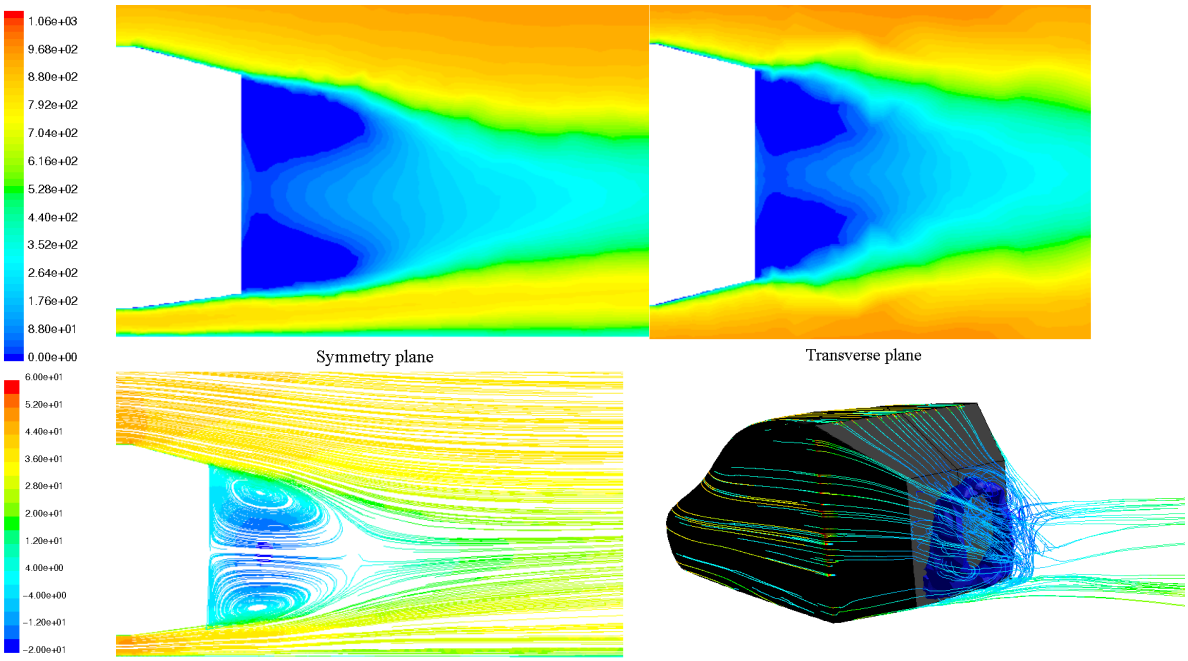

Figure 6: 3D vehicle-like body wake for $(\alpha\ ;\ \beta\ ;\ \gamma) = (14.5\ ;\ 7.6\ ;\ 14.3)$.
Top: contour of total pressure on the symmetry plane (left) and on the middle transverse plane (right). *Bottom*: path line on the symmetry plane coloured by longitudinal velocity (left) and on the rear coloured by velocity magnitude (right).

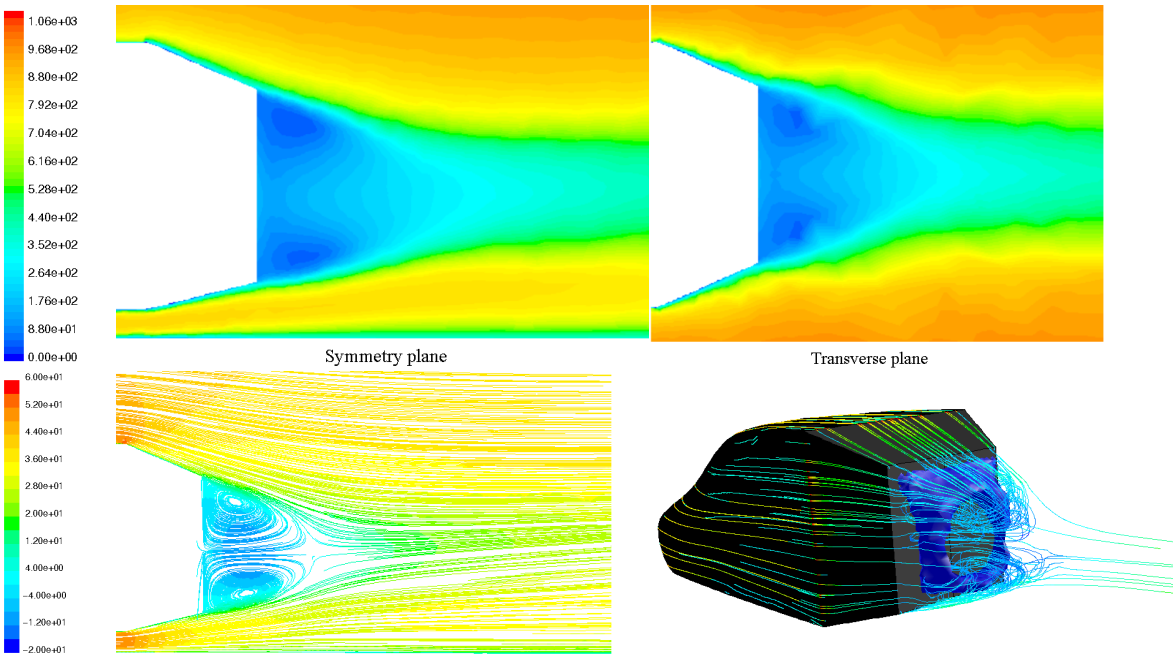

Figure 7: 3D vehicle-like body wake for $(\alpha\ ;\ \beta\ ;\ \gamma) = (23.1\ ;\ 13.6\ ;\ 23.3)$.
Top: contour of total pressure on the symmetry plane (left) and on the middle transverse plane (right). *Bottom*: path line on the symmetry plane coloured by longitudinal velocity (left) and on the rear coloured by velocity magnitude (right).